Table 2 Response time and thrust coefficient due to turbulence[a]

Type	V, m/sec	τ, chords	$\tau c/L$	$\bar{C}_T$, $\bar{w}_g$ = 1m/sec	$\bar{C}_T$, 2m/sec	$\bar{C}_T$, 4m/sec
Soaring glider	22.0	12.0	0.028	0.00032	0.0013	0.0050
Light airplane	30.9	13.2	0.066	0.00030	0.0012	0.0049
Fighter	105.0	99.5	0.829	0.00016	0.00063	0.0025
Transport	64.7	35.8	0.417	0.00024	0.00098	0.0039

[a] $L = 300$ m, $C_L = 1.0$ (sea level).

$\alpha/\alpha_g = A(\tau'\omega) + iB(\tau'\omega)$. Substituting these values in Eq. (3) for the mean thrust coefficient gives:

$$\bar{C}_T = \frac{K\bar{w}_g^2}{\pi V^2} \int_0^\infty \frac{1+3K_1^2}{(1+K_1^2)^2} (A^2+B^2)\,dK_1 \qquad (4)$$

where A and B must be expressed in terms of the nondimensional frequency K_1. Since A and B are functions of $\tau'\omega$, and $\tau'\omega = (\tau c/V)(K_1 V/L) = (\tau c/L)K_1$, the quantity under the integral sign is a function of the parameter $\tau c/L$. Physically, this quantity represents the ratio of the distance for subsidence of the airplane motion to the scale of turbulence.

Results and Discussion

A plot of the integrand of Eq. (4) as a function of K_1 for various values of the parameter $\tau c/L$ is shown in Fig. 1. The value of the integral, labeled thrust factor, F, as a function of $\tau c/L$ is shown in Fig. 2. As shown in Fig. 1, for all except very small values of $\tau c/L$, most of the thrust comes from low frequency components of turbulence, and the area under the curve is not much affected by the upper frequency limit assumed. For very small values of $\tau c/L$ (less than 0.02) however, the contributions to the thrust are nearly uniform throughout the frequency range. The effect of unsteady lift and spanwise gust variations, which attenuate the lift variations at high frequencies, was approximated by taking the upper frequency limit of the integration as $K_1 = 20\pi$.

To show the significance of the results given in Fig. 2, calculations have been made for several typical airplane types having the characteristics given in Table 1. The estimated values of thrust coefficient due to flight through turbulence having scale length L of 300 m and root-mean-square gust velocities of 1, 2, and 4 m/sec are shown in Table 2. These values are shown for a lift coefficient of 1.0 at sea level. The values of thrust coefficient vary directly with lift coefficient because of the effect of lift coefficient on airspeed and hence on the term $\bar{w}_g^2/V^2$. The thrust coefficient, therefore, decreases at higher flight speeds. The thrust coefficient has been found to be little affected by increasing altitude for the soaring glider and the light airplane, but to decrease with increasing altitude for the fighter and transport.

In the case of lightly loaded airplanes flying at low airspeed, the angle-of-attack variation due to gusts, $\bar{w}_g/V$, is relatively large, but the short response time constant of these airplanes allows them rapidly to assume the vertical velocity of the surrounding air mass, thereby reducing the thrust contributions of low-frequency gusts which contain most of the energy of turbulence. More heavily loaded airplanes, on the other hand, produce less attenuation of the effects of the low-frequency gusts, but because of their higher airspeed, the value of $\bar{w}_g/V$ in turbulence of a given intensity is reduced. As shown by Table 2, the resulting effect is to give about the same relatively low value of thrust coefficient for each of the airplane types in flight at given values of lift coefficient and turbulence intensity.

In conclusion, the thrust effects due to turbulence vary as the square of the turbulence intensity and are quite small for moderate turbulence. Only for rather severe turbulence are the effects large enough to be given any consideration. In the case of a soaring glider in turbulence with a root-mean-square velocity of 4 m/sec, the thrust coefficient due to the turbulence at $C_L = 1.0$ is about 0.005. For typical soaring gliders, the value of L/D at $C_L = 1.0$ might range from 20 to 40. The thrust coefficient is therefore from 10 to 20% of the drag coefficient of the glider. In view of the large disturbances of the flight path in turbulence of this magnitude, it is doubtful that the effect would be noticeable.

References

[1] Katzmayr, R., "Effect of Periodic Changes of Angle of Attack on Behavior of Airfoils," TM147, Oct. 1922, NACA.

[2] Davenport, W. B., Jr. and Root, W. L., *An Introduction to the Theory of Random Signals and Noise*, McGraw-Hill, New York, 1958, Chap. 12, formula (12-23), p. 225.

Prediction of Span Loading from Measured Wake-Vortex Structure —An Inverse Betz Method

Vernon J. Rossow*
NASA Ames Research Center, Moffett Field, Calif.

Introduction

A THEORETICAL tool frequently used to study the circumferential velocity distribution in lift-generated vortices is the simple rollup method of Betz.[1] His theory is based on the conservation equations for inviscid, two-dimensional vortices and predicts the circulation in the fully-developed vortex from the span loading on the generating wing. This relationship between span loading and vortex structure is extended here by introducing a so-called inverse rollup method that predicts the span loading on the generating wing when the radial distribution of circumferential velocity in the vortex is given. After the equations to be used in the theory are derived, several examples are presented wherein measured circumferential velocities in several vortices are used with the inverse method to infer the span loading that produced the vortices. These span loadings are compared with those predicted by vortex-lattice theory for the generating wing.

Derivation of Inverse Rollup Method

As mentioned in the Introduction, the existing or direct Betz method[1] for the structure of fully-developed vortices is based on the conservation laws for two-dimensional vortices; i.e., conservation of circulation and of the first and second moments of circulation. To achieve a unique result, the vortex sheet is assumed to roll up in an orderly fashion from the wing tip inboard so that successive layers of the sheet are wrapped around the center and over previous wrappings (Fig. 1 of Ref. 2). Any axial or streamwise variation in the flow velocity is

Received November 4, 1974; revision received January 24, 1975.

Index categories: Aircraft Aerodynamics (including Component Aerodynamics); Jets, Wakes, and Viscid-Inviscid Flow Interactions; Aircraft Flight Operations.

*Staff Scientist. Associate Fellow AIAA.

assumed to have a negligible effect on the rollup process. Equivalent simplified forms of the original Betz formulation appear to have been made at about the same time by Donaldson et al.,[3] Jordan,[4] and Rossow.[2]

The inverse rollup method introduced here is based on the same assumptions as the direct Betz method. The derivation is begun with the expression that relates the radius r_1 in the vortex to the spanwise station on the wing y_1 which contains a given amount of circulation. From Eq. (12) of Ref. 2, the relationship between r_1 and y_1 for the right wing can be written as

$$r_1 = -\frac{1}{\Gamma_w(y_1)} \int_{b/2}^{y_1} \Gamma_w(y)\,dy \qquad (1)$$

Since the circulation in the vortex $\Gamma_v(r_1)$ contained within the radius r_1 is equal to that shed by the wing between its tip at $b/2$ and y_1, the conservation of circulation yields $\Gamma_v(r_1) = \Gamma_w(y_1)$. Equation (1) can then be written as

$$\frac{d}{dr_1}[r_1\Gamma_v(r_1)] = -\frac{d}{dr_1}\int_{b/2}^{y_1}\Gamma_w(y)\,dy$$

$$= -\Gamma_w(y_1)\frac{dy_1}{dr_1}$$

so that

$$-\frac{dy_1}{dr_1} = 1 + \frac{r_1}{\Gamma_v(r_1)}\frac{d\Gamma_v(r_1)}{dr_1}$$

On integration, one form of the inverse relationship between y_1 and r_1 is derived as

$$\frac{b}{2} - y_1 = r_1 + \int_0^{r_1} \frac{r}{\Gamma_v(r)}\frac{d\Gamma_v(r)}{dr}\,dr \qquad (2)$$

A simpler form of Eq. (2) can be derived by use of the fact that the vortex is axially symmetric so that the circulation may be written as $\Gamma_v = 2\pi r_1 v_\theta$, so that, in terms of measured quantities,

$$(b/2) - y_1 = r_1 + \int_0^{r_1} [d(rv_\theta)/v_\theta] \qquad (3)$$

Near the vortex where $v_\theta \approx r\cdot\text{const}$ (which corresponds to the vicinity of the wing tip), Eq. (3) becomes

$$\left[\frac{b}{2} - y_1\right]_{y_1 - b/2} = r_1 + \int_0^{r_1}\frac{d(cr^2)}{cr} = 3r_1$$

Similarly, outside the vortical region where $(v_\theta)_{r_1 \geq r_{max}} = \Gamma_v/2\pi r_1$,

$$\left[\frac{b}{2} - y_1\right]_{y_1 \approx 0} = r_1 + \int_0^{r_{max}}\frac{d(rv_\theta)}{v_\theta} = r_1 + \text{const}$$

where r_{max} is the radius that contains all the vorticity shed by the right wing.

Region of Applicability of Rollup Theories

The simplicity of both the direct and present inverse rollup methods results from the assumptions that the vortex is completely rolled up and that the rollup process is inviscid. These two assumptions then limit the downstream interval over which the theories apply. The upstream end of the region of applicability begins where the rollup of the vortex sheet is largely completed and can be estimated by use of inviscid, time-dependent rollup calculations. Results such as those in Figs. 6 and 10 of Rossow[5] indicate that a major part of the rollup process behind many wings can be considered as practically complete within 3-5 span lengths behind the generating wing.

The downstream end of the region of applicability is the distance at which viscous and turbulent decay of the vortex has modified its structure to the extent that the inviscid theory no longer approximates it. An estimate for this limit can be obtained from the recent data of Ciffone and Orloff[6] wherein a so-called plateau region is identified. Within this plateau region, they found that the vortex decays very little, but it is followed by a region where the vortex decays roughly as $t^{-1/2}$. These considerations suggest that the region of applicability of the Betz method lies between about 5 span lengths and the downstream end of the plateau region, which is estimated from the data of Ciffone and Orloff.[6] Another consequence of the inviscid rollup assumption is that excessively high

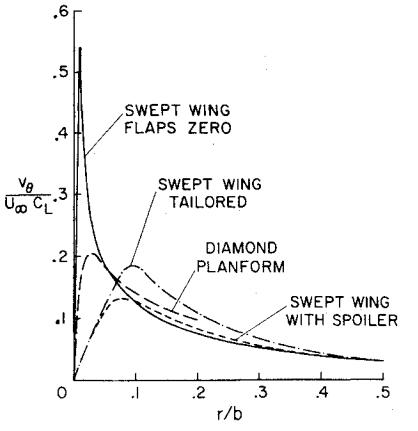

Fig. 1 Measured vortex velocity profiles used in the inverse rollup theory for span loadings. Diamond planform data from Ref. 6 and swept wing data from Ref. 8.

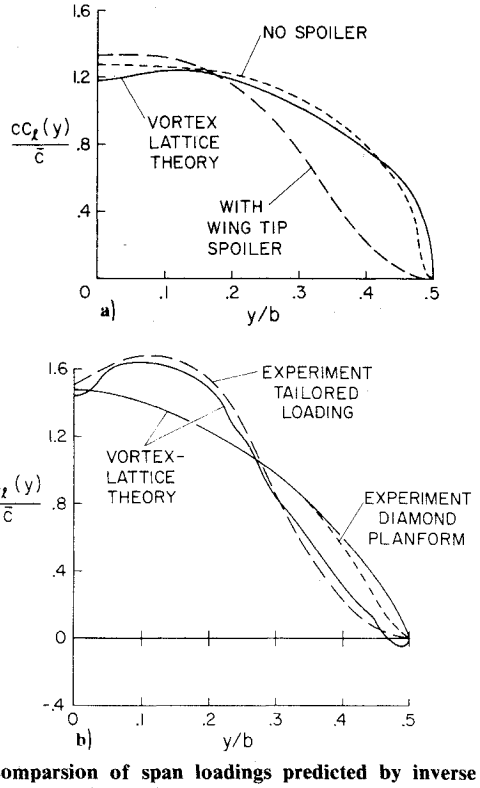

Fig. 2 Comparsion of span loadings predicted by inverse rollup theory (using data from Fig. 1) with vortex-lattice theory; a) swept wing with flaps not deflected and b) diamond planform wing and swept wing with flaps deflected in tailored configuration.

velocities are often predicted at and near the center of the vortex. Nevertheless, comparisons made by Donaldson et al.[3,7] have shown that, outside the core region (radius of maximum circumferential velocity), the Betz rollup theory yields reliable estimates for the vortex structure.

Sample Cases Using Inverse Rollup Method

The span loadings calculated from Eq. (3) and some of the measured vortex data given in Refs. 6 and 8 are now compared with the span loadings predicted by a vortex-lattice theory developed by Hough[9] and adapted† to the model wings of Refs. 6 and 8. The data from Ref. 6 were taken while a wing of diamond planform of 0.609 m (2 ft) span, and an aspect ratio of 5.33 was towed through a water channel. The velocity data were taken with a two-component laser velocimeter. The velocity data in Ref. 8 were taken with a three-component hot-wire probe at the end of a rotating boom. This second wing had a span of 1.84 m, an aspect ratio of 5.9, and the 30% chordline was swept 35.° Each side of the wing had seven flap segments that could be deflected individually in 5° increments. The tests were conducted at a freestream velocity of 40 m/sec corresponding to a Reynolds number of 843,000. Measurements were made in the wake at 13.5 spans (24.4 m) behind the generating wing. Both sets of data have had the velocity contributions of vortex meander[10] and of the companion vortex in the pair removed so that the velocity distribution is that of an isolated vortex (as assumed in the theory). The reduced vortex velocity data from Refs. 6 and 8 used here are presented in Fig. 1 to illustrate the differences in the various profiles. The reader is referred to Refs. 6 and 8 for the reasons for testing these particular wing configurations.

The results presented in Figs. 2a and 2b show that the inverse rollup theory can recover the span loading on the generating wing fairly accurately. A difference near the wing tip, that will occur with almost all configurations, is caused by the finite core size and solid-body rotation in the vortex near $r=0$. The magnitude of the distortion in span loading depends on the size of the core, which is influenced by the character of the boundary layer on the wing and on the viscous and turbulent shear forces in the vortex itself. In most cases, these distortions appear to be small and to occur only near the wing tip. The case labeled "with wing tip spoiler" in Figs. 1 and 2a was added to demonstrate that turbulence injected into the wake by a spoiler on the upper wing surface causes the inverse rollup method to yield a very different span loading even though the measured lift on the wing is about the same as without a spoiler. Figure 1 indicates that the structure of the vortex was changed by a large amount by the spoiler for $r/b <$ 0.1. This change in circumferential velocity is then reflected in the span loading recovered by the inverse method (see Fig. 2a). These results show that the inverse method is inadequate when devices such as spoilers are used to increase turbulence in the wake.

The foregoing results show that the inverse rollup technique yields a fairly accurate representation of the span loading on the generating wing when turbulence effects are not large. This technique also yields an estimate of the comparable span load required to produce a given vortex structure, which makes it a useful diagnostic tool in wake-vortex research.

†The author thanks O.J. Lemmer for adapting the basic vortex-lattice program to the wings studied here.

References

[1] Betz, A., "Verhalten von Wirbelsystemen," *Zeitschrift fuer Angewandte Mathematik und Mechanik,* Bd. XII, Nr. 3, 1932, pp. 164-174; see also NACA TM 713.

[2] Rossow, V. J., "On the Inviscid Rolled-up Structure of Lift-Generated Vortices," *Journal of Aircraft,* Vol. 10, Nov. 1973, pp. 647-650.

[3] Donaldson, C. duP., Snedeker, R. S., and Sullivan, R. D., "A Method of Calculating Aircraft Wake Velocity Profiles and Comparison with Full-Scale Experimental Measurements," AIAA Paper 74-39, 1974, Washington, D.C.

[4] Jordan, P. F., "Structure of Betz Vortex Cores," *Journal of Aircraft,* Vol. 10, Nov. 1973, pp. 691-693.

[5] Rossow, V. J., "Theoretical Study of Lift-Generated Vortex Wakes Designed to Avoid Roll Up," AIAA Journal, Vol. 12, April 1975, pp. 476-484.

[6] Ciffone, D. L. and Orloff, K. L., "Far-Field Wake-Vortex Characteristics of Wings," *Journal of Aircraft,* Vol. 12, May 1975, pp. 464-470.

[7] Donaldson, C. duP., "A Brief Review of the Aircraft Trailing Vortex Problem," Rept. 155, May 1971, Aeronautical Research Associates of Princeton, Princeton, N.J.

[8] Rossow, V. J., Corsiglia, V. R., Schwind, R. G., Frick, J. K. D., and Lemmer, O. J., "Velocity and Rolling-Moment Measurements in the Wake of a Swept-Wing Model in the 40- by 80-Foot Wind Tunnel," TM X-62,414, April 1975, NASA.

[9] Hough, G., "Remarks on Vortex-Lattice Methods," *Journal of Aircraft,* Vol. 10, May 1973, pp. 314-317.

[10] Corsiglia, V. R., Schwind, R. G., and Chigier, N. A., "Rapid Scanning, Three-Dimensional Hot-Wire Anemometer Surveys of Wing Tip Vortices," *Journal of Aircraft,* Vol. 10, Dec. 1973, pp. 752-757.